# OMAE2021-61663

# UPLIFT CAPACITY OF SUCTION CAISSONS IN SAND FOR GENERAL CONDITIONS OF DRAINAGE

Ragini Gogoi Texas A&M University College Station, Texas Charles P. Aubeny Texas A&M University College Station, Texas Phillip Watson
University of Western Australia
Perth, Australia

Fraser Bransby
University of Western Australia
Perth, Australia

#### **ABSTRACT**

Suction caissons have emerged as a viable solution for the foundations of offshore wind turbines, which are gaining momentum worldwide as an alternate energy source. When used in a multi-bucket jacket system, the system capacity is often governed by the uplift capacity of the windward bucket foundation. Seabed conditions at offshore windfarm sites often comprise dense sand where the soil response may be drained, partially drained or undrained depending on the loading regime, the foundation dimensions and the soil conditions. Given the large difference in uplift capacity of caissons for these different drainage conditions, predicting the behavior of a suction caisson under a range of drainage conditions becomes a paramount concern. Consequently, this paper presents the findings of a coupled finite element investigation of the monotonic uplift response of the windward caisson of a multi-bucket jacket system in a typical dense silica sand for a range of drainage conditions. The study adopts a Hypoplastic soil constitutive model capable of simulating the stress-strain-strength behavior of dense sand. This choice is justified by conducting a comparative study with other soil models – namely the Mohr Coulomb and bounding *surface sand models – to determine the most efficient soil failure* model to capture the complex undrained behavior of dense sand. The numerical predictions made in this study are verified by recreating the test conditions adopted in centrifuge tests previously conducted at the University of Western Australia, and demonstrating that the capacity from numerical analysis is consistent with the test results. The Hypoplastic soil constitutive model also provides an efficient method to produce accurate load capacity transition curves from an undrained to a drained soil state.

Keywords: Suction caisson, Drained, Undrained, Hypoplastic soil model

#### 1. INTRODUCTION

In the context of global warming and rapid depletion of traditional energy resources, research in alternate energy sources is fast becoming a priority, with offshore wind energy proving to be promising. Recent years have witnessed a sudden rise in the construction and development of offshore wind farms worldwide, with the Global Wind Report predicting a 2.7% increase in the market each year.

Suction caissons represent a suitable foundation type for offshore wind turbines (OWTs) supported on jacket structures. Comprising hollow, open ended foundations, they are installed in the seabed partially by their own self-weight and partially due to the application of differential pressure (suction) across the foundation cap [1]. The absence of a hammer during installation, and relatively low steel volumes for the capacity generated, provide caissons with a competitive edge over conventional pile foundations for moderate water depths.

Suction caissons can be designed to resist the forces acting on a typical OWT, comprising relatively light self-weight vertical forces with large horizontal forces and overturning moments induced by wind and wave action [2]. Figure 1 demonstrates the loads acting on a typical OWT and jacket structure. The resisting moment is mostly provided by the vertical reaction of individual caissons in a multi-foundation arrangement, through the development of a push-pull mechanism – caissons in the leeward side develop a compressive axial force whereas the caissons on the windward side develop a tensile axial force [3]. Under extreme offshore storm conditions, the ability of the windward caissons to resist uplift is a dominant foundation consideration, and the tensile capacity of a caisson under severe pull-out conditions must be evaluated accurately. Since a significant fraction of the tensile capacity of a suction caisson relies on transient negative excess pore pressures ('suction'), potential dissipation of suction within the time duration of individual loads must be well understood.

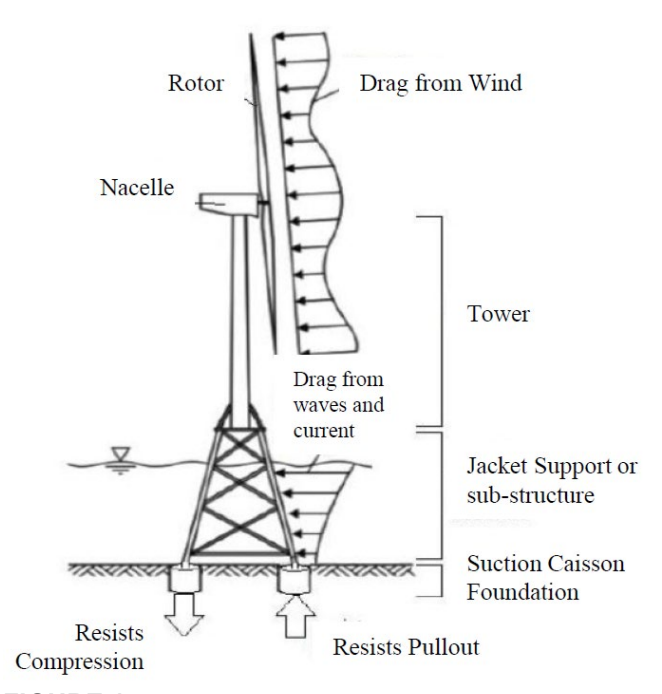
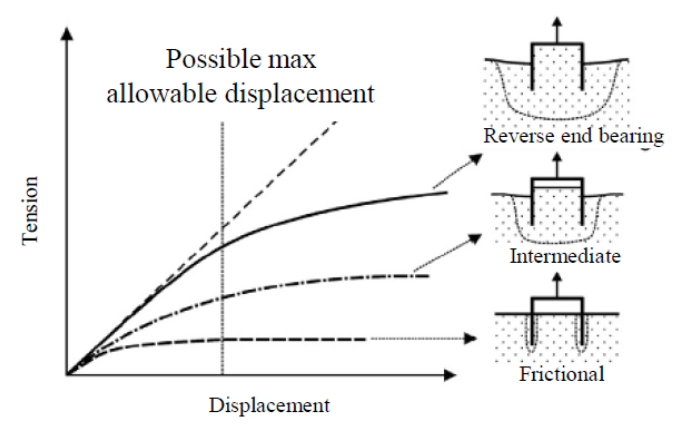


FIGURE 1: LOADS ON AN OWT [12]

This paper presents a numerical study simulating the response of the trailing suction caisson in a jacket arrangement subject to monotonic, purely vertical pull-out under a range of drainage conditions. Noting that the dissipation of suction is governed by the process of soil consolidation, the range in drainage condition studied are characterized by the usual parameters known to control this process: rate (or duration) of loading, soil coefficient of consolidation  $(c_v)$ , and size of the foundation [4].



**FIGURE 2:** FAILURE MECHANISMS OF A SUCTION CAISSON IN DENSE SAND SUBJECTED TO A MONOTONIC UPLIFT [5]

The response of a caisson subjected to uplift under fully drained conditions is described as 'frictional', and under fully undrained conditions as 'reverse end bearing'. In contrast, partial drainage conditions lead to intermediate behavior [5]. Components of frictional resistance include the caisson buoyant weight - controlled by the difference between the unit weight of steel and

the unit weight of the soil - and the skin friction mobilized along the outer and inner surfaces of the caisson skirt. On the other hand, undrained uplift occurs at a much faster rate than the rate of dissipation of suction, resulting in the generation of significant (negative) pore pressure at the soil-caisson interface below the top cap. As a result, the entire soil mass within the caisson is mobilized during the loading – resembling the behavior of a soil plug. Additional resistance is realized by mobilizing soil beneath and outside the caisson [6], creating a 'reverse end bearing' mechanism that provides the strongest resistance to an uplift loading. Figure 2 demonstrates the failure mechanisms described.

This study has focused on University of Western Australia (UWA) superfine silica sand at a relative density of 90%, which is considered to be a broad representative of offshore sands found at OWT locations, including in the North Sea and the US East Coast [7,8].

#### 2. NUMERICAL MODEL

#### 2.1 General

A finite element model was developed to study the response of a suction caisson installed in sand and subjected to monotonic tensile loading, thereby simulating the windward caisson in a multi-bucket jacket. A fully-coupled model was utilized, which allows for the transient analysis of a partially or fully drained porous medium and adopts effective stress principles to describe its behavior. The analysis was performed with the software package Abaqus [9]. The model comprises of a rigid, impermeable skirted foundation wished-in-place in an isotropic soil with a stress dependent Young's Modulus, E. The finite element mesh generated is presented in Figure 3.

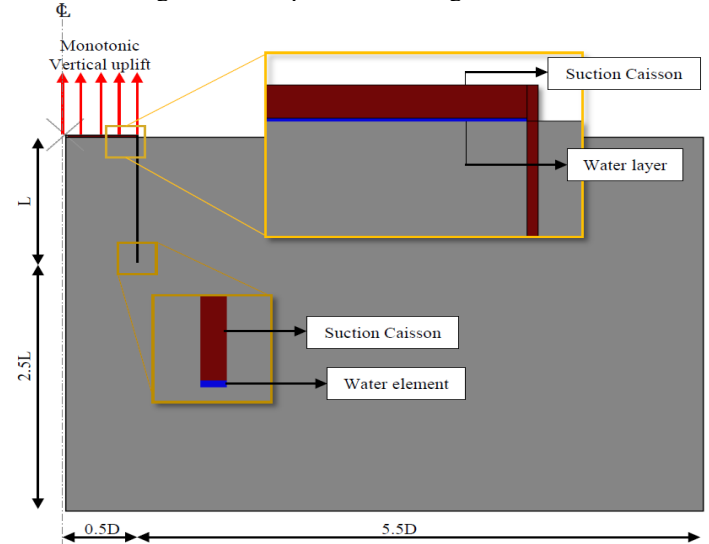


**FIGURE 3:** AXISYMMETRIC MODEL OF A SINGLE SUCTION CAISSON FOUNDATION (D=6m, L=6m)

The analysis was able to utilize axisymmetry due to the cylindrical caisson geometry and the axisymmetric (vertical) loading. Consequently, the soil medium is meshed using fournode axisymmetric, displacement and pore-pressure elements of

type CAX4P, from the element library available in ABAOUS/Standard. The size of the soil domain is set at 3.5 times the length and 6 times the diameter of the bucket to minimize boundary effects. At the bottom of the domain, movement is restrained in both the vertical and radial directions. while only radial movement is restricted on the vertical boundaries. The seepage path is defined by controlling the pore pressure degree of freedom for the nodes at the boundary of the model. Drainage is allowed at the top surface of the model surrounding the caisson, the far field boundary and the bottom boundary but the axis of symmetry is modelled impermeable.

The suction caisson itself, of diameter D, length L and wall thickness t, is modelled using 'impermeable' CAX4 type elements. The elements are given an elastic modulus of 70 GPa and Poisson's ratio of 0.3. The geometries simulated in the current study are listed in Table 1.

**TABLE 1:** GEOMETRY OF SUCTION CAISSON

Diameter	Length	Aspect Ratio	Skirt Thickness
D (m)	L (m)	(L/D)	t (mm)
6	6	1	30
8	4	0.5	50

Interaction along the caisson skirt with the soil was described using the isotropic Coulomb friction model, with the coefficient of friction defined as:

$$\mu = \tan(\varphi_{in}) \tag{1}$$

 $\mu = \tan(\varphi_{in}) \tag{1}$  where the interface friction angle  $\varphi_{in}$  was obtained from laboratory tests for the soil type and skirt wall roughness under consideration (Table 2). An additional condition of no separation was applied to the interface between the inner wall of the skirt and the soil [10]. This prevented numerical convergence problems when running the model for large displacements, required to mobilize the full undrained capacity.

Monotonic tensile loading was applied using displacement control where the caisson was subjected to constant velocity uplift until a vertical displacement of 1% the caisson diameter was achieved. Different drainage conditions were simulated in the numerical model by controlling the pull-out rate of the caisson. A slow uplift, allowing sufficient time for the excess pore pressure developed in the soil to dissipate completely, simulates drained loading. In contrast, rapid uplift or pull-out will not provide the required time for the pore pressures to dissipate, thus creating partially to undrained loading conditions.

#### 2.2 Water Element

Accurate representation of the transfer of load from the topcap of the suction caisson to the soil was ensured by modelling the area beneath the top cap with a thin layer (10 cm) of elements with negligible shear stiffness.

This layer was assigned physical properties representative of water [6, 10, 11]. The primary function of this layer was to allow even distribution of suction over the top-cap of the caisson, while also enabling a gap to form below the top-cap during partially drained to drained loading. As noted by Mana [10], the water elements do not undergo immediate volume change during loading, but will instead produce excess pore pressure within the elements – achieved by adopting a stiffness of 10E-8 kN/m<sup>2</sup> and Poisson's ratio of 0.499 [7]. Their permeability was set much higher than the soil body to ensure uniform distribution of pore pressure throughout the layer. A single element of similar properties was also generated at the tip of the caisson skirt.

**TABLE 2**: SOIL PROPERTIES FOR UWA SUPERFINE SILICA **SAND** 

PARAMETER	VALUE
Bulk density, D <sub>R</sub>	90%
Buoyant unit weight, γ'	$10.6 \text{ kN/m}^2$
Initial void ratio, e	0.535
Coefficient of earth pressure at	0.344
rest, k <sub>o</sub>	
Wall friction angle, $\phi_{int}$	20.951°
Initial permeability, k <sub>ini</sub>	1.09x10 <sup>-4</sup> m/s

# 2.3 Soil constitutive modelling

This current study employed the rate dependent Hypoplastic soil model by von Wolfersdorff [13] to accurately capture the behavior of dense sand under different drainage conditions. Model parameters are related to the granulometric behavior of the soil, making it a preferred material law for modelling granular soil. It is described by a non-linear tensorial equation, which accounts for the dilatancy, barotropy and the pyknotropy of the soil [6].

The proposed hypoplastic constitutive equation (after [13]) is written as:

$$\dot{T} = L(T, e): D + N(T, e)||D||$$
 (2)

where the objective stress rate,  $\dot{T}$ , is a tensorial function of the Cauchy stress, T, stretching rate, D, and void ratio, e; with L and N as second order linear and fourth order non-linear constitutive tensors, respectively.

This model describes the post-yield behavior of dense sand, and is able to account for dilatancy and the stress path dependent stiffness of the soil. Unlike elastoplastic soil models, no distinction of elastic and plastic deformation, yield and plastic potential surfaces or hardening rules are needed. The absence of these mathematical notions serves as an advantage for hypoplastic models over more widely used elastoplastic models.

An additional advantage of the model is its easily derivable 8 parameters, of which the critical state friction angle  $(\varphi_c)$  is the only material constant required [13]. The granulate hardness ( $h_s$ ) and exponent (n) take into account the influence of compression and can be determined by conducting an oedometer test at an initially loose soil state, reflecting the slope and curvature of the compression curve respectively [14]. The model parameters can be approximated using the following equations [14]:

$$n = 0.366 - 0.0341 \left( \frac{c_u}{\left( \frac{d_{50}}{d_0} \right)^{0.33}} \right) \tag{3}$$

$$h_s = 3p_s \left(\frac{ne_p}{C_c}\right)^{1/n} \tag{4}$$

where,  $C_u$  is the non-uniformity coefficient,  $d_{50}$  is the mean grain size and  $d_0 = 1$  mm. In Equation 4,  $C_u$  is the compressibility coefficient for loose sand and  $e_p$  and  $p_s$  are the void ratio and corresponding pressures from the oedometer test data. The maximum  $(e_{i\theta})$ , minimum  $(e_{d\theta})$  and critical  $(e_{c\theta})$  void ratios at zero pressure are based on the maximum, minimum and critical void ratio. A reasonable assumption of their values are as follows [14]:

$$e_{do} \approx e_{min}$$
;  $e_{co} \approx e_{max}$ ;  $e_{io} \approx 1.2e_{max}$  (5)

The exponent ( $\alpha$ ) controls the dependency of the peak friction angle on the void ratio, while  $\beta$  relates the relative density to the soil stiffness [15], and can be calculated using the following equations [14]:

$$\alpha = \frac{\ln\left[6\frac{(2+K_p)^2 + a^2K_p(K_p - 1 - tanv_p)}{a(2+K_p)(5K_p - 2)\sqrt{4 + 2(1 + tanv_p)^2}}\right]}{\ln\left(\frac{e - e_d}{e_c - e_d}\right)}$$
(6)

with the peak ratio,

$$K_p = \frac{1 + \sin \varphi_p}{1 - \sin \varphi_n}$$

$$\tan vp = 2\frac{K_p - 4 + 5AK_p^2 - 2AK_p}{(5K_p - 2)(1 + 2A)} - 1$$

with,

$$A = \frac{a^2}{(2 + K_p)^2} \left[ 1 - \frac{K_p(4 - K_p)}{5K_p - 2} \right]$$

and,

$$a = \frac{\sqrt{3}(3 - \sin\varphi_c)}{2\sqrt{2}\sin\varphi_c}$$

The void ratios,  $e_d$  and  $e_c$  in the denominator of Equation 6 correspond to the mean effective pressure at peak state and are approximated using [14]:

$$\frac{e_d}{e_{do}} = \frac{e_c}{e_{co}} = exp\left[-\left(\frac{3p_s}{h_s}\right)^n\right] \tag{7}$$

The soil properties required for the above equations can be attained by conducting a triaxial test at a dense soil state. The value for the last parameter,  $\beta$  was assumed as 1 as an initial approximation and then calibrated to best fit lab test data. The mathematical equations required for their determination are explained in detail by Herle at al. [14].

The model parameters adopted in this study, along with the soil properties for UWA superfine silica sand are listed in Table 3 and Table 2 respectively. The hypoplastic soil model was implemented in Abaqus via a User Subroutine written in FORTRAN by Felin et al. [16], available in Soilmodels [17].

For comparison purposes, finite element analyses have also been carried out using the ABAQUS in-built Mohr-Coulomb soil failure model, with a non-associative flow rule and constant values of soil friction and dilation angle. The Mohr-Coulomb model is a widely accepted model and was selected due to its mathematical simplicity and the clear physical meaning of its parameters. The undrained behavior of dense sand is strongly influenced by the dilation of the soil, making it crucial for the model to capture this behavior accurately. Though a nonassociative flow rule allows the dilation angle to be restricted, the absence of a means to cap the dilation generated by the model causes it to predict constant dilation throughout plastic loading. This implies the soil will continue to dilate infinitely as shearing progresses [18]. This does not represent real soil behavior, which after significant shearing, will reach a state of constant volume or critical state condition. Thus, unrealistically high undrained strength or capacity can be expected from the model. The parameters used in this model were derived from laboratory tests conducted at UWA, with the fiction angle taken as 41° and dilation angle as 10°. The elastic behavior is defined by the Young's modulus of elasticity, which has been derived in terms of a soil rigidity index  $(I_r)$ , which is calculated from the relative density  $(D_r)$  and confining stress  $(\sigma_c)$  [19]:

 $I_r = (aD_r + b)[m_0 + m_1log(\sigma'_c) + m_2log^2(\sigma'_c)]$  (8) The variables in the equation are detailed in Al Hakeem and Aubeny [19].

**TABLE 3:** HYPOPLASTIC MODEL PARAMETERS

PARAMETER	VALUE
Critical state friction angle, φ <sub>c</sub>	33.1°
Granular hardness, h <sub>s</sub>	61000 MPa
Exponent, n	0.2657
Minimum void ratio, e <sub>do</sub>	0.5
Critical void ratio, e <sub>co</sub>	0.84
Maximum void ratio, eio	1.008
Exponent, α	0.06
Exponent, β	0.5

#### 3. RESULTS: HYPOPLASTIC SOIL MODEL

A suction caisson with diameter and skirt length of 6 m (aspect ratio = 1), and wall thickness of 30 mm was modelled as a reference case in the current study. Simulations were performed for tensile displacement rates in the range of 0.005mm/s to 500 mm/s, until the caisson reached a targeted uplift of around 1% of its diameter, thereby replicating a range in drainage conditions within the soil. The pull-out behavior of the caisson, and the generation of excess pore pressure, for each simulation (using an initial void ratio of 0.535 and permeability of 1.09E-04 m/s) is described and compared with theoretically predicted responses in the following sections. The upift resistance calculated does not include the weight of the caisson which was modeled as neutrally buoyant.

Figure 4 shows the variation of uplift capacity (with vertical load, V normalized by foundation projected area, A (=  $\pi D^2/4$ )) with uplift displacement (U) for different loading rates, illustrating the expected trend of increasing capacity as pull-out rate increases.

Drained loading (representative of sustained uplift loading) was modelled by applying a slow pull-out rate of 0.005mm/s.

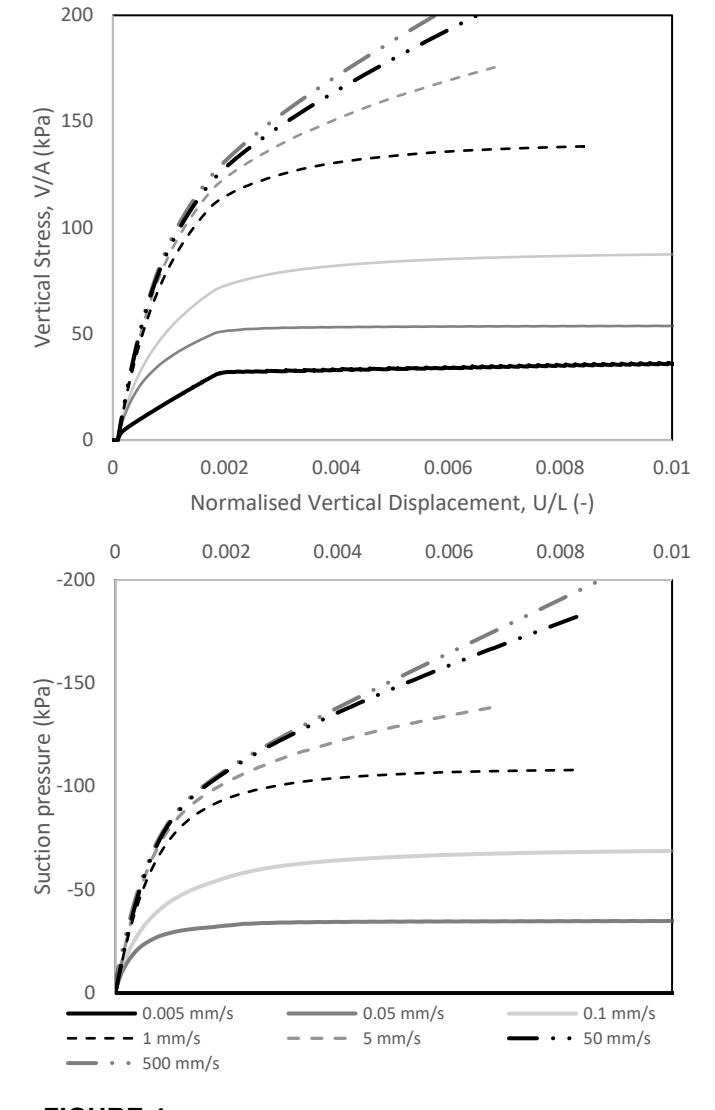


**FIGURE 4:** VERTICAL STRESS-DISPLACEMENT CURVE AND SUCTION PRESSURE-DISPLACEMENT CURVE FOR THE REFERENCE SYSTEM

The bilinear load-displacement curve indicates that resistance is due to skin friction only [6], which agrees with the displacement contours (Figure 5A) within the mesh also, illustrating a failure mechanism similar to Figure 2. The FEA predicted capacity of 35.87 kPa agrees to within 7% with analytical equations in Houlsby et al. [20] for pure friction.

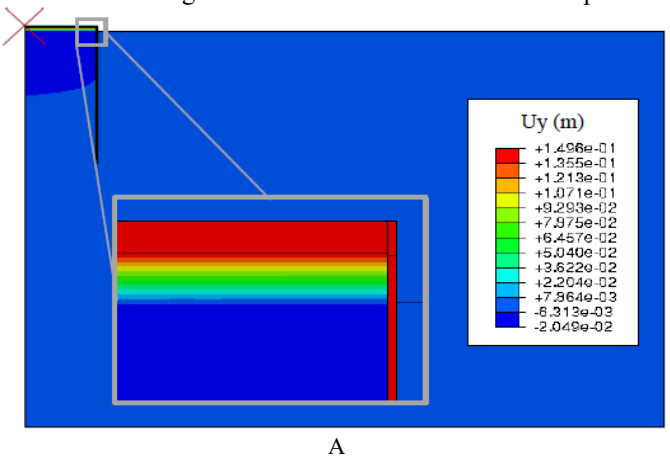
As the pull-out rate increases, the vertical resistance increases drastically. For loading at rates above 10 mm/s, the ultimate capacity was not attained even for the targeted uplift of 0.01D, indicating that large displacements are needed to mobilize the full undrained capacity. A maximum loading rate of 500 mm/s was selected, since further increases resulted in negligible differences to the load-displacement curve. The displacement contours (Figure 5B) for the fully undrained case (500mm/s) shows an uplift in the soil within the caisson along with it, thus demonstrating a 'reverse end bearing' behavior.

The suction response follows a similar trend to that of the load-displacement curve as described above. Figure 4 also shows the variation of suction pressure within an element below the top cap, which represents the suction generated during different loading conditions. For fully drained loading, no excess pore pressure is generated. In contrast, significant suction is mobilized for fully undrained conditions, resulting in the entire soil mass inside the caisson undergoing vertical upward displacement, and the soil outside the caisson to move inward (and down). The net vertical displacement of the soil inside and outside the caisson was observed to be 0±4.3%, as it should be for fully undrained (constant volume) conditions. This suction pressure generated at the interface of the caisson top cap and the soil body controls the water depth required to avoid cavitation [6]:

$$\Delta u < u_c + \gamma_w * h_w \tag{9}$$

where the cavitation pressure ( $u_c$ ) is set as the atmospheric pressure (-100 kN/m²) and the unit weight of water ( $\gamma_w$ ) can be approximated as 10 kN/m³. The limiting water depth ( $h_w$ ) was estimated to be 31.8 m for a displacement of 0.01D.

Partial drainage conditions exhibit intermediate responses.



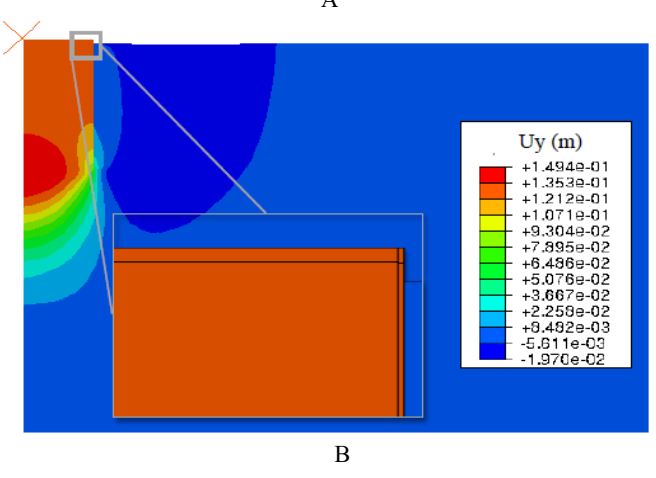


**FIGURE 5:** VERTICAL DISPLACEMENT CONTOURS AND EXPANSION OF THE WATER LAYER BENEATH THE CAISSON TOP CAP, A) FULLY DRAINED CONDITION, B) FULLY UNDRAINED CONDITION

#### 4. VALIDATION STUDIES

The current study has been validated by comparing the findings to available model test results. Successful numerical simulations conducted by Whyte et al. [7] using a bounding surface soil model and centrifuge model tests conducted by Senders [5] and Bienen [21] provide a base to evaluate the accuracy of the Hypoplastic soil model in predicting the drained to undrained behavior of dense sand.

# 4.1 Comparison with Whyte's numerical study

The transition curves obtained from the current study were compared against similar curves produced by Whyte [7], where a bounding surface constitutive model for sand was used based on the Manzari-Dafalias model architecture. The model requires a total of nineteen parameters, with a detailed explanation of calibration of the model parameters provided in [7].

The transition curves represent the variation of the axial capacity with the drainage condition of the soil expressed in terms of a normalized time factor (T):

$$T = \frac{c_v t}{D^2} \tag{10}$$

where t is the loading duration, D is the diameter of the caisson and  $c_v$  is the (vertical) coefficient of consolidation of the soil, based on the estimated permeability and the estimated constraint modulus [7]. The vertical loads required for different caisson uplift displacements are presented in Figure 6 compared to previously published data. The graph shows that the Hypoplastic model predictions are in agreement with previous analysis. For smaller time factors, i.e., short term or undrained loading, the Hypoplastic model predictions somewhat exceed the capacities predicted in [7]. However, with increasing time duration of loading (i.e., the transition toward drained behavior) the differences decrease.

# 4.2 Comparison with centrifuge model tests

Senders conducted a number of centrifuge model tests to investigate the behavior of caissons subject to uplift loading in sand. These tests used UWA superfine silica sand (with an initial void ratio of 0.535 and permeability of 1.09E-04 m/s) and used model dimensions resulting in equivalent dimensions to the reference case in the current study. Loading rates of 0.1 mm/s

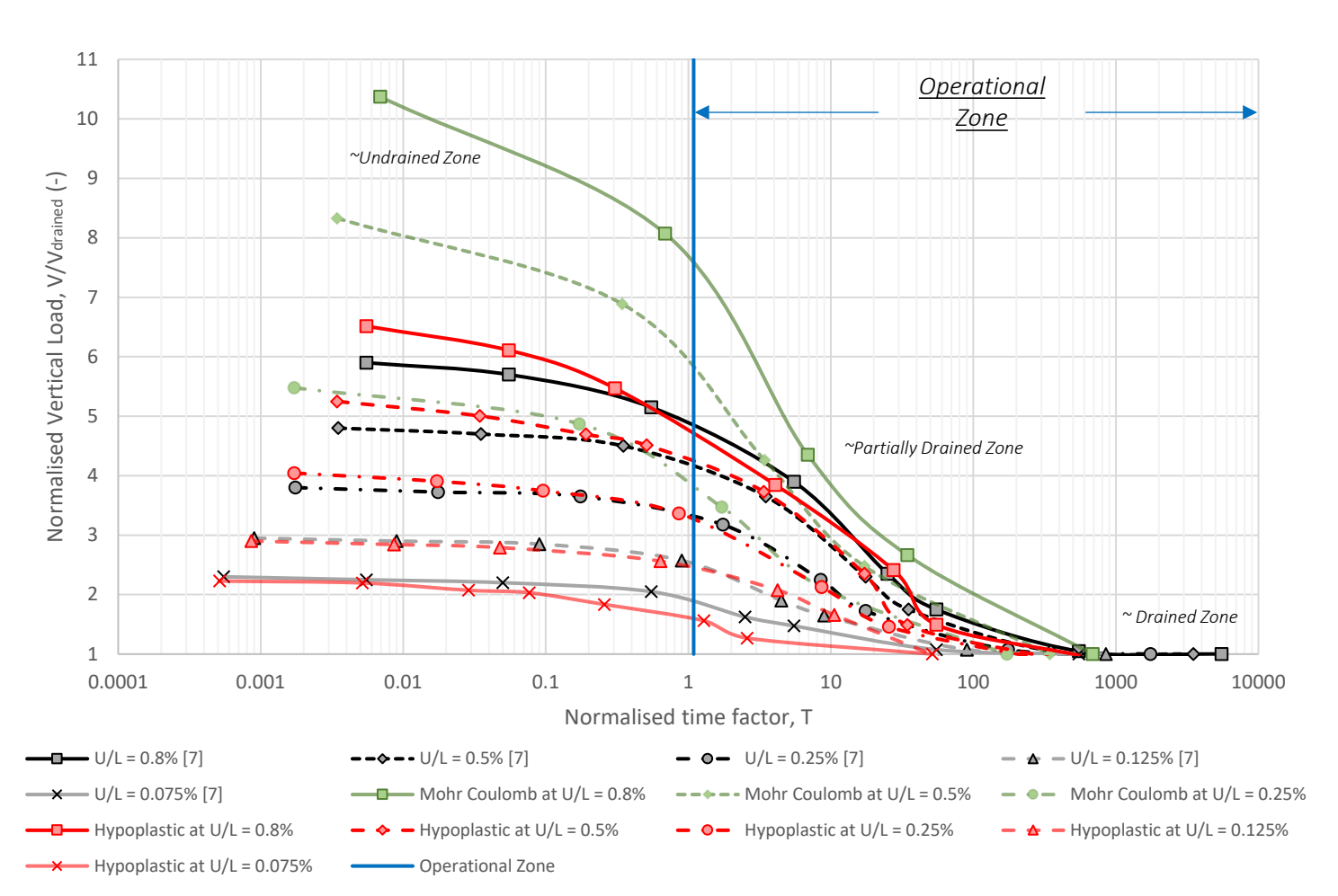


**FIGURE 6:** TRANSITION CURVE FOR REFERENCE SYSTEM: PREDICTIONS BY BOUNDING SURFACE MODEL [7], MOHR COULOMB MODEL AND HYPOPLASTIC MODEL

and 0.5mm/s were selected to simulate a drained behavior and partially drained behavior respectively [5].

A fully (or close to) undrained centrifuge test at a loading rate of 3 mm/s was conducted by Bienen [21]. This test was performed using Baskarp sand, with relative density of 95%, initial void ratio of 0.57 and permeability of 1.22E-05 m/s. While not modelled directly, it is believed that due to its similar particle size distribution, the soil properties adopted for UWA superfine silica sand are broadly representative. Consequently, additional FE analyses were conducted for this condition using the same soil parameters used in the current study and the resulting load-displacement curves for the comparative study are presented in Figure 7C.

The drained and the undrained FEA provide acceptable predictions against the measurements, but the numerical results on Figure 7B underestimate the partially drained capacity (at 0.007D) by 13.1% at a loading rate of 0.5 mm/s.

The initial response of the FEA for the drained (Figure 7A) and the partially drained analyses is stiffer than the centrifuge results. A possible explanation for this is faster mobilization of excess pore pressure in the FEA than the physical tests [7].

# 5. COMPARISON OF SOIL MODELS

In order to justify the use of a complex Hypoplastic soil constitutive model, repeat analysis was performed in the current study with the Mohr Coulomb soil model – allowing direct comparison of analysis with the Hypoplastic model, the Mohr Coulomb model and Whyte's bounding surface sand model.

The predictions are compared with the centrifuge model tests conducted by Senders [5] and Bienen [21] in Figure 7. The Mohr Coulomb model, with Young's modulus as proposed in AlHakeem and Aubeny [19], compared well with centrifuge data for the initial elastic responses across all drainage conditions.

In comparison with predictions of ultimate capacity under fully drained conditions based on Houlsby's analytical method [20], errors in prediction of 10.3% for the Mohr Coulomb model, 12.9% for Whyte's bounding surface model, and 6.66% for the Hypoplasticity model are noted. Thus, the Hypoplastic model appears well suited for predicting completely drained response. This is further observed in Figure 7 at a loading rate of 0.1mm/s, described by Senders [5] as fully drained, whereby the Hypoplastic model provides the best match with the centrifuge results, considering a balance between the initial and ultimate responses.

For a partially drained condition of 0.5mm/s loading rate, as shown in Figure 8, the Hypoplasticity model and the Mohr Coulomb model underestimate the ultimate capacity (at 0.007D) by 13.1% and 5.5%, respectively. Further, they do not follow the trends observed in the centrifuge test, with capacity increasing with displacement, which is successfully modeled by Whyte's bounding surface model.

The Mohr Coulomb model drastically overestimates the fully undrained capacity (at loading rate 3mm/s) since dilation significantly influences the undrained behavior, and this is uncapped in the Mohr Coulomb model. Both the Hypoplastic

model and Whyte's Bounding surface sand model accurately follows the path of Bienen's test in Figure 7.

Figure 6 shows the Mohr Coulomb results in the form of a transition curve, as described in Section 5.1, to further compare the three soil models. Though the results are fairly similar for the longer loading durations (drained behavior), when compared with Figure 6, for short-term loading the capacities deviate significantly.

Overall, it is reasonable to conclude that the Hypoplastic model provides useful predictions for caisson behavior under vertical uplift loading in dense sand. It is in generally good agreement with Whyte's somewhat more complex model in its prediction of the load capacity, capturing the transition from drained to undrained loading conditions. Further, it has the added advantage of requiring only 8, easily derivable parameters; in contrast to the 19 required by the bounding surface model.

It should be noted that the current study restricts the uplift of the caisson to only 1% of the diameter, in contrast to 2% reported in other studies [6]. The next section looks into the allowable displacement for a suction caisson supporting an offshore wind turbine subjected to a purely monotonic uplift.

#### 6. PRACTICAL CONSIDERATIONS

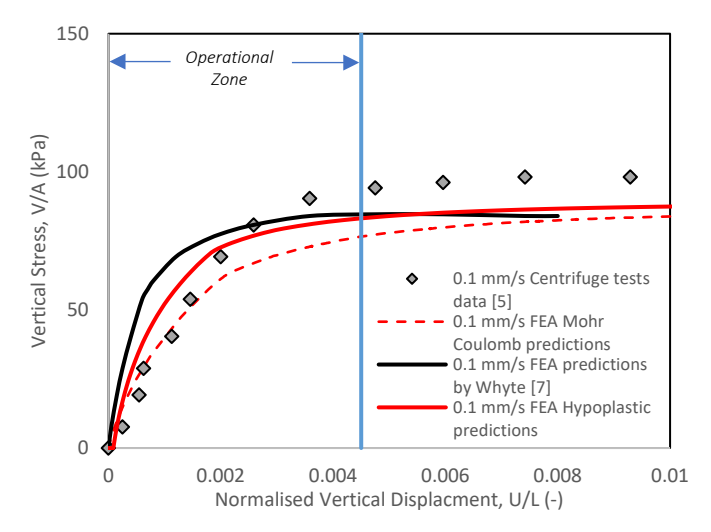
The aim of the current study was to predict the capacity of the windward suction caisson of a multi-bucket jacket structure, supporting an offshore wind turbine in dense sand. Over the lifespan of an OWT, it may be subjected to various offshore environmental conditions – both from wind and wave loading, which can be categorized on the basis of their time periods. Data suggests an extreme wind (gusts) and wave loads lasts for 10.5 seconds and 12 seconds [5], respectively. Thus, a limiting time period of 10.5 seconds is considered relevant to represent a 'typical' extreme storm condition. The range suggested by extreme loading periods is shown against the transition curves presented in Figure 6 (for the soil  $c_v$  and foundation sizes investigated) via a blue vertical line, with the starting time factor in the range (operational zone) depicting a storm condition and the higher times, steading conditions.

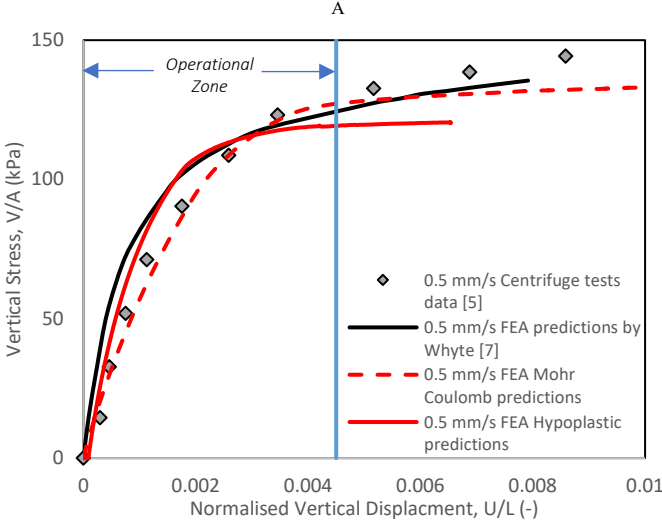
Another factor narrowing the range of interest for practical application of OWT foundations is the allowable displacement.

Data suggests the maximum allowable tilt for an OWT after installation to be between 0.003 to 0.009 radians [22]. For typical jacket configurations, this produces an uplift of 0.17% to 0.45% of the diameter of the suction caisson – well within the testing limit of 1% adopted for the current study. The range limited by the maximum allowable displacement is shown by a vertical blue line in Figure 7.

# 6.1 Resistance against environmental loads

For illustrative purposes, a 3 MW OWT that is 86 m high and supported in a water depth of 25 m by a tripod jacket with caissons spaced at around 22 m from the column of the OWT is considered. Although smaller than many of the turbines currently being installed, this was chosen to fit the conditions numerically investigated in this paper and validated against previously-conducted centrifuge test results [5, 21]. The total weight of





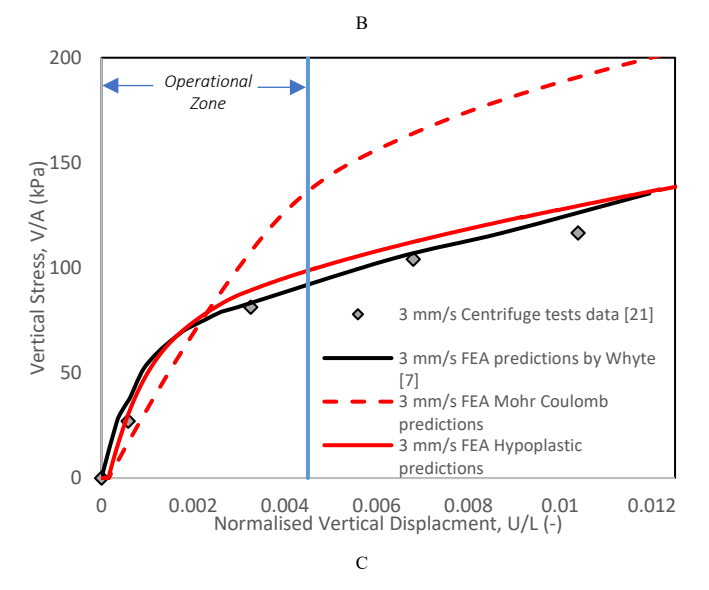


**FIGURE 7:** LOAD DISPLACEMENT OF THE REFERENCE SYSTEM AT DIFFERENT LOADING RATES

the structure is estimated to be around 7 MN, and is initially distributed equally over each caisson [5].

For a wave height of 9 m and period of 11.1 s, such an OWT will achieve an overturning moment of 155 MN-m [5], and the restoring moment will be produced due to the push-pull mechanism of the vertical loads on the caissons as described earlier.

To attain this moment, the required tensile capacity was calculated to be 2.367 MN using the following equation, [5]:

$$M_R = (1.5 * V_T + 0.5 * W)s_t$$
 (11) where s<sub>t</sub> is the spacing between the center of the wind turbine and the center of each of the three member caissons, W is the total

the center of each of the three member caissons, W is the total weight of the turbine, including the caissons and  $V_T$  is the tensile capacity.

From Equation 10, a time factor (T) of 0.6 is calculated for this wave period and consolidation coefficient of UWA superfine silica sand, as used in this paper. The corresponding tensile capacity was 4.5 MN from Figure 6, at a displacement of 0.5%D. This provides a factor of safety of 1.9. Based on this, the current FE model (using the Hypoplasticity constitutive model) is capable of successfully predicting the behavior required to resist failure [23].

Figure 7 allows a wave period of 11.1 s to be categorized as undrained loading. This is largely dependent on the coefficient of consolidation of the soil. A high value of time factor, T represents a loading condition where full drainage is allowed to occur, which results in lower and unacceptable factors of safety. Lower time factors represent undrained conditions, with their higher tensile capacities and thus acceptable factors of safety.

### 7. CONCLUSION

A numerical study was undertaken to simulate the response of a trailing caisson in a tripod jacket supporting an OWT, in UWA Superfine Silica Sand at a relative density of 90%. A monotonic, purely vertical uplift was adopted as the testing load since previous studies had established the tensile capacity of the windward caisson to be the critical design load condition. Different drainage conditions varied from fully undrained to fully drained to represent the various offshore environmental conditions.

A hypoplastic soil model [13] was adopted for the FE analyses conducted. Its parameters are closely related to the granulometric behavior of the soil, providing convenient material law for modelling granular soil. The predictions of the FEA using this model were compared against the predictions made with Mohr Coulomb as the failure model, and results from a published study using a bounding surface sand model; as well as against published centrifuge model test results.

The study showed that for normal offshore environmental conditions, represented by a long-term loading, or fully drained loading, the Hypoplastic failure model provides the closest match to the capacity predicted analytically [20], with an error percentage of only 6.66%. Thus, for fully drained capacity, the Hypoplastic model is recommended.

In an extreme storm condition, represented by a short-term loading, or fully undrained condition, the Hypoplastic model provided accurate matches to the centrifuge results, and additionally due to its relatively simple parameters, was preferred. For a partially drained condition, comparisons to centrifuge test data and predictions by the Whyte bounding surface model show the Hypoplastic model to underestimate capacity. However, the Hypoplastic model prediction of the transition in uplift capacity from drained to undrained loading compares well with the bounding surface model.

The current FEA with the Hypoplastic soil model also predicted a FOS of 1.9 for the resisting moment for a 3 MW OWT, 86 m high, supported by a tripod suction caisson foundation system. Thus, it successfully provides sufficient resistance to uplift against failure and further reinforces the established capability of suction caissons as a viable foundation option to support offshore wind farms.

#### **ACKNOWLEDGEMENTS**

The third and fourth authors are (respectively) supported by the Shell Chair in Offshore Engineering and the Fugro Chair in Geotechnics at UWA, which are (respectively) sponsored by Shell Australia and Fugro. The first two authors would also like to acknowledge the support from National Science Foundation, award number CMMI-1936901 and the Texas A&M High Performance Research Computing facility for the use of their resources in running the numerous finite element analyses supporting this study.

#### **REFERENCES**

- [1] Aubeny, C., 2018, Geomechanics of Marine Anchors, Boca Raton: CRC Press.
- [2] Byrne, B., 2000, "Investigations of suction caissons in dense sand", Ph.D., University of Oxford.
- [3] Bransby, F., and Martin, C., 1999, "Elasto-plastic modelling of bucket foundations", International Symposium on Numerical Models in Geomechanics (NUMOG), pp. 425-430.
- [4] Vaitkunaite, E., Nielsen, B., and Ibsen, L., 2016, "Bucket Foundation Response Under Various Displacement Rates", International Journal of Offshore and Polar Engineering, 26(2), pp. 116-124.
- [5] Senders, M., 2008, "Suction Caissons in Sand as Tripod Foundations for Offshore Wind Turbines", Ph.D., The University of Western Australia. School of Civil and Resource Engineering.
- [6] Thieken, Klaus & Achmus, Martin & Schröder, Christian, 2014, "On the behavior of suction buckets in sand under tensile loads," Computers and Geotechnics, 60, pp. 88–100.
- [7] Whyte S, Burd HJ, Martin CM, Randolph MF, Bienen B, Rattley M, Roy A, Stapelfeldt M, "Comparison of numerical simulations using a bounding surface model to centrifuge tests of axial loaded suction buckets in dense sand" (Under-review)
- [8] Low, H.E., Zhu, F., Mohr, H., Erbrich, C., Watson, P., Bransby, F., O'Loughlin, C., Randolph, M., Mekkawy, M., Travasarou, T., O'Connell, D., and Zhang, Z., 2020, "Cyclic Loading of Offshore Wind Turbine Suction Bucket Foundations in Sand: The Importance of Loading Frequency", International Symposium on Frontiers in Offshore Geotechnics, DFI, Austin

- [9] Dassault Systems, 2012. Abaqus analysis user's manual. USA: Simulia Corporation.
- [10] Mana DS, Gourvenec S, Randolph MF., 2014, "Numerical modelling of seepage beneath skirted foundations subjected to vertical uplift," Computers and Geotechnics, 55, pp. 150-157.
- [11] Achmus, M., & Thieken, K., 2014, "Numerical Simulation of the Tensile Resistance of Suction Buckets in Sand," Journal of Ocean and Wind Energy, 1(4), pp. 231-239.
- [12] Nikitas, G., Vimalan, N., and Bhattacharya, S., 2016, "An innovative cyclic loading device to study long term performance of offshore wind turbines", Soil Dynamics and Earthquake Engineering, 82, pp. 154-160.
- [13] von Wolffersdorff, P.-A., 1996, "A hypoplastic relation for granular materials with a predefined limit state surface," Mech. Cohes.-Frict. Mater., 1, pp. 251-271.
- [14] Herle, Ivo & Gudehus, Gerd., 1999, "Determination of Parameters of a Hypoplastic Constitutive Model from Properties of Grain Assemblies," Mechanics of Cohesive-frictional Materials.
- [15] Stutz, Hans & Wuttke, Frank, 2018, "Hypoplastic modelling of soil-structure interfaces in offshore applications," Journal of Zhejiang University.
- [16] Fellin, W. and Ostermann, A., 2002. Consistent tangent operators for constitutive rate equations. *International Journal for Numerical and Analytical Methods in Geomechanics*, 26(12), pp.1213-1233.
- [17] Fellin, Wolffersdorff and Roddeman. *UMAT Implementation of Sand Hypoplasticity by UIBK SoilModels*. SoilModels. Available at:

https://soilmodels.com/download/umat-hyposand-uibk/

- [18] Wood, D., 2009, Soil Mechanics: A One-Dimensional Introduction, Cambridge: Cambridge University Press.
- [19] Al Hakeem, N., and Aubeny, C., 2019, "Numerical Investigation of Uplift Behavior of Circular Plate Anchors in Uniform Sand", Journal of Geotechnical and Geoenvironmental Engineering, 145 (9).
- [20] Houlsby, G. T., Kelly, R. B., & Byrne, B. W., 2005, "The tensile capacity of suction caissons in sand under rapid loading,". Proceedings of the International symposium on frontiers in offshore geotechnics, Perth, Australia, pp. 405-410.
- [21] Bienen, B., Klinkvort, R., O'Loughlin, C., Zhu, F., and Byrne, B., 2018, "Suction caissons in dense sand, part I: installation, limiting capacity and drainage", Géotechnique, 68(11), pp. 937-952.
- [22] Malhotra, S., 2011, "Selection, Design and Construction of Offshore Wind Turbine Foundations," Wind Turbines, Dr. Ibrahim Al-Bahadly (Ed.), ISBN: 978-953-307-221-0, InTech.
- [23] American Bureau of Shipping, 2013, Guide for Building and Classing: Floating offshore wind turbine installations.